From local to global: Cortical dynamics of contour integration

Topi Tanskanen Brain Research Unit, Low Temperature Laboratory, Helsinki University of Technology, Espoo, Finland

Jussi Saarinen Department of Psychology, University of Helsinki, Helsinki, Finland

Lauri Parkkonen Brain Research Unit, Low Temperature Laboratory, Helsinki University of Technology, Espoo, Finland

Riitta Hari Brain Research Unit, Low Temperature Laboratory, Helsinki University of Technology, Espoo, Finland, & Department of Clinical Neurophysiology, Helsinki University Central Hospital, Helsinki, Finland

Processing of global contours requires integration of local visual information. To study the involvement of different cortical areas and the temporal characteristics of their activity in such integration, we recorded neuromagnetic responses to arrays of Gabor patches in which a proportion of the patches was oriented either tangentially or radially with respect to a global circular contour; arrays with random patch orientations served as control stimuli. The first responses at 60–80 ms around the calcarine sulcus were similar to all stimuli. Starting from 130 ms, responses to the tangential contours differed significantly from responses to control stimuli, and the difference reached its maximum at 275 ms. The most pronounced differences emerged around the parieto-occipital sulcus, precuneus, cuneus, and superior and middle occipital gyri. This pattern of cortical activity was similar irrespective of whether the local elements were radial or tangential to the circle; however, the differences were smaller for the radial contours and tended to start 20–30 ms later. Correspondingly, discrimination reaction times were shortest for the contours consisting of tangential elements. These results demonstrate two spatially and temporally distinct stages of visual cortical processing, the first one limited to local features and the second one integrating information at a more global level.

Keywords: perceptual organization, shape and contour, visual cortex, functional imaging, magnetoencephalography, human

Citation: Tanskanen, T., Saarinen, J., Parkkonen, L., & Hari, R. (2008). From local to global: Cortical dynamics of contour integration. *Journal of Vision, 8*(7):15, 1–12, http://journalofvision.org/8/7/15/, doi:10.1167/8.7.15.

Introduction

The Gestalt school formulated as early as 70 years ago perceptual laws that describe how the visual percept emerges from local elements to more global shapes and objects (Koffka, 1935). However, the neural mechanisms underlying these processes still remain a subject of extensive research (Hess, Hayes, & Field, 2003; Roelfsema, 2006; Sasaki, 2007).

Neurons in the earliest stages of cortical visual processing have well-characterized selectivity for spatial frequency and orientation. Neurons in the primary visual cortex (V1) have small receptive fields (RFs; Hubel & Wiesel, 1974), but stimuli that surround the classical RF can modulate their responses and also affect the perceived orientation and contrast (Kapadia, Ito, Gilbert, & Westheimer, 1995; Knierim & van Essen, 1992). The initial 50-ms response of monkey V1 cells to oriented line segments is affected only by the stimulus part landing on the neuron's classical RF, whereas a later sustained response, starting around 80–100 ms, emerges when the receptive field is on the border of two texture surfaces (Lamme, 1995; Rossi, Desimone, & Ungerleider, 2001; Zipser, Lamme, & Schiller, 1996).

Corresponding behavioral effects have been demonstrated in humans. Field, Hayes, and Hess (1993) introduced an influential paradigm to study how perception of global forms and contours depends on the properties and organization of their constituent local elements: When contours consisting of Gabor patches are embedded within arrays of randomly oriented similar patches, they are detected most efficiently when the orientations of the local elements match the orientation of the global contour (Bonneh & Sagi, 1998; Field et al., 1993; Kovács & Julesz, 1993; Pettet, McKee, & Grzywacz, 1998; Saarinen & Levi, 2001; Saarinen, Levi, & Shen, 1997).

Functional magnetic resonance imaging (fMRI) has pinpointed areas involved in contour processing (Altmann,

doi: 10.1167/8.7.15 Received October 13, 2007; published June 30, 2008 ISSN 1534-7362

Bülthoff, & Kourtzi, 2003; Dumoulin & Hess, 2007; Kourtzi, Tolias, Altmann, Augath, & Logothetis, 2003) but has been unable, due to its limited temporal resolution, to unravel the corresponding time courses.

To study the involvement of different cortical areas and the temporal characteristics of their activity in processing required for contour integration, we recorded cortical responses with whole-scalp magnetoencephalography (MEG; Hämäläinen, Hari, Ilmoniemi, Knuutila, & Lounasmaa, 1993) when the subjects were viewing arrays of Gabor patches (Marcelja, 1980), a portion of which either did or did not form a circular contour. This setup provided a strong version of the path stimuli introduced by Field et al. (1993). The stimulus display time was set to 0.5 s to clearly exceed the 0.15- to 0.25-s time needed for saturation of contour detection (Braun, 1999; Hess, Beaudot, & Mullen, 2001).

Our main interest was to find out when the cortical responses to contour and no-contour stimuli would differ from each other; we also aimed at identifying the sites of early contour-specific activity and to study the effect of the local orientation of elements on the cortical responses.

Methods

Subjects

Eight healthy members of laboratory personnel (4 females and 4 males; mean age 27 years, range 24–33; 7 right-handed and 1 ambidextrous; normal or corrected-to-normal visual acuity) were studied after written informed consent. The MEG recordings had a prior approval by the Ethics Committee of the Helsinki and Uusimaa Hospital District.

Experimental setup

Stimuli

The stimuli were square arrays of 120–140 Gabor elements (Figure 1), presented to the center of the visual field. In the no-contour stimuli, all elements were oriented randomly and positioned pseudorandomly without overlap. In the contour stimuli, about one fourth (36/140) of the elements were oriented and positioned so that they formed an easily detectable double circle. Because a single cell in the primary visual cortex is most sensitive to approximately one element (Marcelja, 1980), the first cortical responses to both contour and no-contour stimuli should be similar since the global variables—such as luminance, contrast, element density, spatial frequency, and orientation distribution—were identical for both stimulus types. In the first condition, the orientations of the contour elements were tangential with respect to the circle and radial in the second condition. In the third condition, the contour consisted of only one quadrant (lower left) of a full circle.

Elements

The stimulus images were generated before the experiments with NIH Image program (developed at the U.S. National Institutes of Health, available at http://rsb.info.nih.gov/nih-image/). The luminance distribution [$G(x, y)$] of each Gabor element was described by the product of a circular Gaussian and an oriented sinusoid:

$$G(x,y) = c\cos\left(2\pi\frac{x\cos\theta + y\sin\theta}{p} + \phi\right)\exp\left(-\frac{x^2+y^2}{2\sigma^2}\right), \quad (1)$$

where σ is the standard deviation of the Gaussian envelope, θ is the orientation and p is the period of the modulating sinusoid, ϕ is the phase of the grating at the center of the envelope, and c is the Michelson luminance contrast.

We kept σ fixed at 6 pixels (0.1 deg). The period p was 12 pixels (i.e., the carrier spatial frequency of each Gabor patch was 4.8 cycles/deg), and the spatial frequency full bandwidth (specified at half of the peak amplitude) was 1.1 octaves. The phase ϕ of the cosine function was set to 0, yielding even-symmetric elements. The Michelson contrast (c) of the elements' luminance was 57%, and the average luminance was equal to that of the gray background, 89 cd/m^2.

Contours

The contour elements were placed on two circular paths, the centers of which lay at the fixation point in the center of the display area. The radii of the paths were 1.56 and 2.19 deg, and the full circles comprised 15 and 21 evenly spaced elements, respectively. The orientation change between neighboring elements was 24.0 deg in the inner and 17.1 deg in the outer circle, and the positions and the orientations of the contour elements had no jitter. The quadrant stimuli comprised 4 elements in the inner circle and 5 elements in the outer circle.

Background

For placing the background elements, the stimulus area (7.56 deg × 7.56 deg) was divided into 12 × 12 slots of 36 pixels × 36 pixels (0.63 deg). A randomly oriented Gabor patch was placed to each slot that was not occupied by a contour element. In the control stimuli, all slots were filled with randomly oriented elements. To pseudorandomize the element positions, the element centers were placed from −14 to 14 pixels (0.24 deg, even distribution) off from the center of the slot, both horizontally and vertically. As a result, densities or orientations of the elements did not differ systematically between contour and no-contour stimuli. Four elements around the fixation

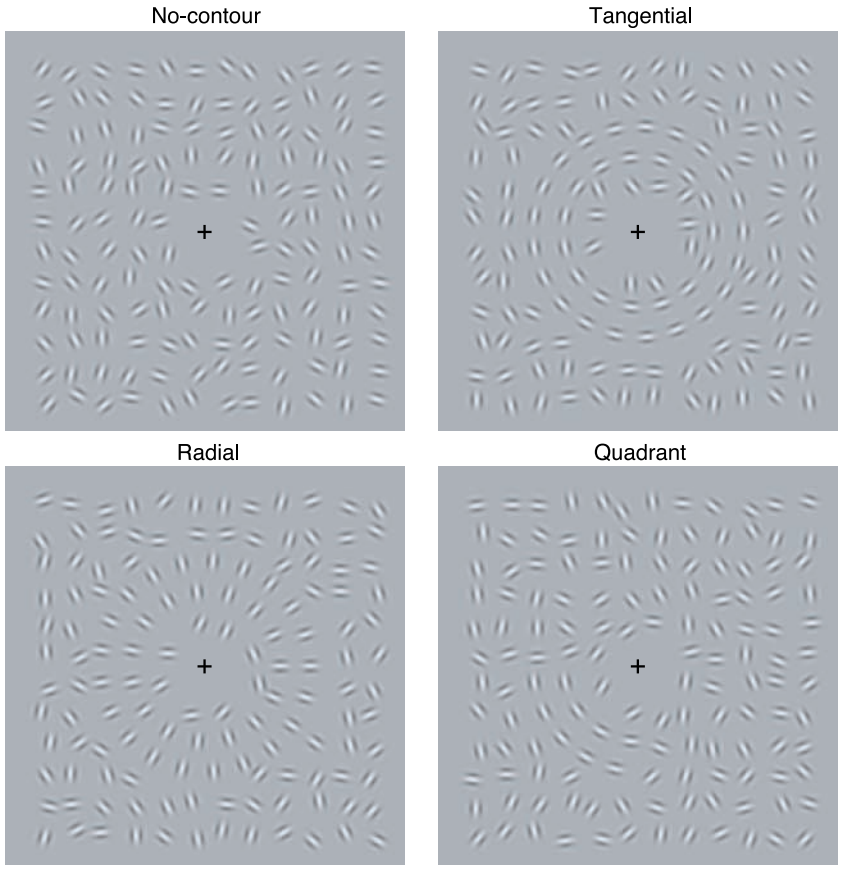

Figure 1. Examples of stimuli. From top left: no-contour and tangential, radial, and quadrant contour stimuli.

point were omitted. For each 3 conditions, 5 contour and 5 no-contour images were generated. The fixation cross was located in the center of the display area.

Equipment

Stimulus presentation was controlled by Presentation® software (http://www.neurobs.com/) run on a PC computer. The stimuli were displayed on a rear projection screen (Dataplex 735-DP50) by a data projector (VistaPro™, Christie Digital Systems Inc., Cypress, CA, USA), based on Digital Light Processing™ and hosting three digital micromirror panels. Thus, the luminance onsets and the offsets were symmetric and abrupt, and all three colors were drawn simultaneously (for details on the projector performance, see Packer et al., 2001). The experiments were run in standard VGA mode (resolution 640 × 480 pixels, frame rate 60 Hz, 256 gray levels).

The subjects viewed the screen binocularly at a distance of 120 cm in a dimly lit room. At this distance, the 23.3-cm × 17.4-cm display area corresponded to 11 deg × 8.25 deg visual angle. The high luminance of the projector was attenuated to an average luminance of 89 d/m^2 by placing a 1.4 log unit neutral density filter in front of the lens. The non-linearity of the luminance response of the projector was corrected during stimulus generation by using the inverse function of the luminance response (gamma correction).

Procedure

The stimuli were presented once every 2.5 s for 0.5 s with abrupt on- and offsets. Subjects were asked to view the stimuli and fixate on a constantly present black cross (2 cd/m^2, 0.17 deg × 0.17 deg) on a gray background.

Each recording block consisted of contour trials (47%), no-contour trials (47%), and catch trials (6%) presented in a random order. In the catch trials, included to maintain and monitor the subjects' vigilance level, the stimuli were replaced with a question mark, and the subject had to report with left/right index finger lifts whether a contour or a no-contour stimulus was presented in the preceding trial. Whether left- and right-sided movements referred to contour or no-contour stimuli was counterbalanced across subjects. Signals from the catch trials were not analyzed. The subjects practiced the task before the first recording blocks until they felt confident about their performance.

Different contour types were presented in separate blocks; two blocks for each type were recorded using an ABCCBA design. The order of conditions was counterbalanced across subjects.

MEG recording

Whole-scalp neuromagnetic signals were measured in a magnetically shielded room while the subject was sitting with the head leaning against the measurement helmet of the Vectorview™ 306-channel magnetometer (Neuromag Ltd., Helsinki, Finland; currently Elekta Neuromag Oy). The helmet-shaped detector array comprises 102 identical SQUID-based triple sensor units, each housing two planar first-order gradiometers and one magnetometer. The two gradiometers of each unit measure orthogonal tangential derivatives of the magnetic field component approximately normal to the head surface.

MEG signals were filtered to 0.1–172 Hz and sampled at 600 Hz. Signals were averaged over a time window starting 0.3 s before and ending 1.0 s after the onset of the stimulus. Horizontal and vertical electro-oculograms were recorded for on-line rejection of epochs contaminated by blinks and eye movements. At least 60 responses to both contour and no-contour stimuli were recorded in each block; thus, a minimum of 120 clean trials were collected for each stimulus type. Each block lasted about 6 min, and the blocks were separated by 2-min breaks.

Before the MEG recordings, four head position marker coils were attached to the subject's scalp. The positions of the coils and three anatomical landmarks (nasion and points immediately anterior to the ear canals) were measured with a 3D digitizer (3Space Fastrak™, Polhemus Inc., Colchester, VT, USA). At the beginning of each recording block, the position of the subject's head with respect to the sensor array was determined. This information was later used to combine the measured neuromagnetic signals with the subject's anatomical MRIs by first identifying the anatomical landmarks in the MR images.

MEG data analysis

The effect of environmental noise on the averaged MEG signals was first attenuated by projecting out the noise subspaces determined from recordings in the absence of the subject (Parkkonen, Simola, Tuoriniemi, & Ahonen, 1999). The responses were digitally low-pass filtered at 35 Hz, and a 300-ms prestimulus baseline was applied for amplitude measurements. To remove drifts during the 1.3-s epochs, a detrending baseline was applied at 800–1000 ms.

Since the effects of interest were very focal, timing was analyzed at sensor level, using signals from the 204 planar gradiometer channels that pick up the strongest signals just above local source currents and thereby give reliable first guesses of the activated brain areas.

The neural generators of the MEG responses were estimated with noise-normalized minimum norm estimates (sometimes referred to as dynamic statistical parametric maps, dSPMs; Dale et al., 2000). The estimate was constrained to the cortex, and source currents normal to the surface of the cortical mantle were favored; this procedure is valid because MEG signals arise mainly from synchronous postsynaptic activity in the apical dendrites of pyramidal cells (Hari, 1990; Okada, Wu, & Kyuhou, 1997).

The current estimates were calculated using the "MNE Software" package (developed by M. Hämäläinen; http://www.nmr.mgh.harvard.edu/martinos/userInfo/data/sofMNE.php). Prior to source estimation, the MEG data were spatially filtered (signal space separation; Taulu, Kajola, & Simola, 2004) to suppress residual external magnetic interference. All the 204 gradiometer and 102 magnetometer signals were included in the analysis. Anatomical magnetic resonance images were processed with the FreeSurfer software (http://surfer.nmr.mgh.harvard.edu/).

A single-compartment boundary element model (BEM) along the inner skull surface was used as the volume conductor. To obtain the source point set, the border between the gray and white matter was tessellated (Dale, Fischl, & Sereno, 1999) and decimated to a 5-mm grid, corresponding to 6000–8700 dipole locations per hemisphere. Dipole amplitudes were determined by an l^2 minimum norm estimate (MNE) that incorporates depth weighting and loose orientation constraints (Lin, Belliveau, Dale, & Hämäläinen, 2006); transverse source current components were weighted by 0.3 with respect to currents normal to the cortical surface. The estimated dipole amplitudes were then normalized by their noise sensitivity, i.e., by the estimated "activity" due to the noise in the measurement. The required noise covariance estimate was obtained from 300-ms prestimulus windows of the unaveraged data. This procedure gave a normalized activity estimate that is t-distributed under the null hypothesis of no responses. With a large number of time points contributing to the noise covariance estimate, the t-distribution approaches the unit normal distribution, i.e., z-score (Dale et al., 2000).

The current estimates were first calculated, for each subject and condition, without taking into account the sign of the current (current in or outward with respect to the cortical surface). The estimates were then spatially smoothed, transformed to the fsaverage atlas brain (provided by the FreeSurfer package) with surface-based morphing (Fischl, Sereno, Tootell, & Dale, 1999) and averaged across subjects.

To find effects consistent across subjects, the smoothed and morphed individual current estimates were also converted into binary maps: For each time instant, a source point was set to 1 if the estimated activity was at least one standard deviation larger to contour than to no-contour stimuli; otherwise, the point was set to 0. This criterion is more conservative than requiring simply larger activity in one condition than another, which would lead to an ordinary binomial test assuming equal probabilities for the events. The binary maps summed across subjects then directly indicated the number of subjects who had a considerably (at least one STD) stronger response to

contour than no-contour stimuli at a given time and cortical location.

Reaction times

After the MEG recording and a rest period of 5–10 min, the subjects participated in a discrimination reaction time (RT) experiment, aimed to provide a coarse measure of the task difficulty in the different conditions. The RTs were collected off-line to avoid movement-related contamination of the MEG data. The stimulus presentation was otherwise identical to that during the MEG recording, but no catch trials were presented. Instead, the subjects responded to each trial as rapidly as possible by lifting the left or the right finger to indicate whether they perceived a stimulus with or without a contour. RTs exceeding ±2.5 STD of the individual RTs were excluded as outliers. At least 20 correct RTs to contour and no-contour stimuli were averaged for each individual and each stimulus category.

Results

Timing of MEG responses to tangential contour vs. no-contour stimuli

Figure 2 (left) shows the spatial distribution of responses of Subject 2 to tangential contour (red) and no-contour (green) stimuli. The first responses occurred in the posterior channels close to the midline. Because of their similarity to both contour and no-contour stimuli, we will refer to them as "non-selective"; in this subject these responses peaked at 76 ms and were followed by a second peak at 106 ms (insert a). The responses to contour and no-contour stimuli started to differ at 96 ms (meaning that their difference exceeded 2 STD of the prestimulus signal), and the difference reached its maximum at 224 ms (insert b). Such differences (contour > no-contour) will be referred to as "contour-sensitive responses."

In all subjects, the sensors picking the early non-selective response were located around the posterior midline (Figure 2c, red squares). The non-selective responses started to exceed the prestimulus noise level at 69 ± 2 ms (mean ±*SEM* across subjects), with a peak at 85 ± 3 ms (for individual latencies, see the "First" values in Figure 4).

For further analysis of the contour-sensitive responses, the channel with the largest peak amplitude was selected from a set of channels that showed sustained differences exceeding 2 STD of the prestimulus noise level. The search covered the entire epoch, i.e., no further latency criteria were applied. However, the same channels also showed the earliest reliable differences between the contour and the no-contour responses. These sensors had a similar or slightly more dorsal distribution than the sensors picking up the early non-selective responses (Figure 2c, blue circles).

Figure 2d shows for all subjects the contour-sensitive responses, i.e., the difference between responses to contour and no-contour stimuli, and Figure 2e illustrates their mean. Across subjects, the difference exceeded the prestimulus noise level by 2 STD at 130 ± 9 ms. Within subjects, the contour-sensitive activity started 61 ± 9 ms later than the first, non-specific response ($p < 0.001$). When the starting point was defined as the beginning of a continuous block of statistically significantly different samples, the estimates were ca. 5 ms later. The contour-sensitive effects typically started with a rapidly increasing difference that reached its maximum at 274 ± 35 ms. Thereafter a weaker and slower difference continued until 600–700 ms, i.e., vanishing 100–200 ms after the offset of the stimulus.

Cortical activation sites

Estimates of the cortical activity, averaged across all subjects, depicted the first responses around the calcarine sulcus (Figure 3 left; Talairach coordinates −8 −94 −5 in the left hemisphere and 10 −93 −4 in the right). The activity in this area peaked at 95 ms, which is 10 ms later than the 85-ms peak in single sensors; the likely reason is that the current estimate integrates information across a group of sensors that, by definition, show later peak latencies than the sensors showing responses with earliest latencies. A second peak occurred around 125 ms in the same cortical region. The source estimates of these two first responses did not differ between the contour and no-contour conditions (Figure 3, bottom left).

Instead, clear contour-sensitive activity peaked around 215 ms at several locations in the posterior parieto-occipital (PO) cortex (Figure 3, right). The grand average across all subjects revealed the most prominent differences in responses to contour vs. no-contour stimuli in the medial surface around the PO sulcus and precuneus (Talairach coordinates for the center of gravity: left −19 −68 19, right 16 −61 32). Such activation differences were clear in 7 of 8 subjects. Differences were observed also in occipital areas spanning from cuneus (−9 −100 10) to the middle occipital gyrus (−33 −85 18) in the left hemisphere and from middle occipital gyrus (26 −95 9) to superior occipital gyrus (17 −85 27 and 40 −80 18) in the right hemisphere. These occipital differences were observed bilaterally in all subjects.

Effect of contour type

The contour-sensitive activation started at 130 ± 9 ms (mean ±*SEM*) for the tangential contours, at 164 ± 17 ms

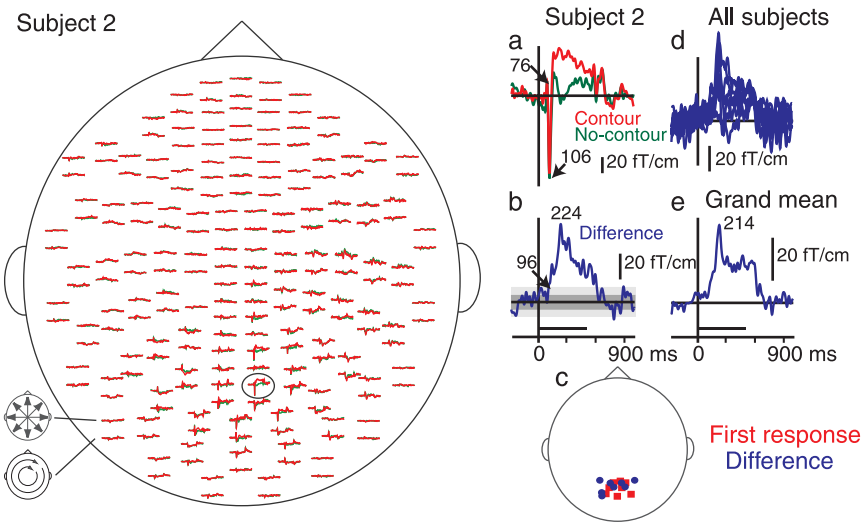

Figure 2. Neuromagnetic responses. Left: responses of Subject 2 to tangential contour (red) and no-contour (green) stimuli. The channel with the earliest and most prominent difference (referred to as contour-sensitive response) is encircled. Inserts: (a) enlarged responses to contour and no-contour stimuli on the encircled channel and (b) the contour-sensitive response. (c) Locations of sensors picking the earliest non-selective responses (red) and earliest contour-sensitive responses (blue) for all subjects. (d) Contour-sensitive traces on the latter (blue) channels for all subjects and (e) their mean. The horizontal black bars under the traces indicate the duration of the stimulus.

for the radial contours, and at 149 ± 13 ms for the quadrant contours (Figure 4). Compared with the onset of the early non-specific responses, the contour-sensitive activity started 61 ± 9 ms later for the tangential contours ($p < 0.001$), 94 ± 16 ms later for the radial contours ($p < 0.01$), and 77 ± 12 ms later for quadrant contours ($p < 0.001$). We did not observe any systematic dependence between response amplitudes and latencies across subjects and contour types. Because the largest amplitude differences between contour and no-contour responses sometimes occurred on different channels than the earliest statistically significant differences, the criteria used to select the channels for the tangential contours were not suitable for conditions with radial and quadrant contours. Therefore, we first identified in the contour-sensitive responses those earliest peaks that were statistically significant on at least 3 neighboring channels. From these, the channel with the largest contour-sensitive response was selected, and the beginning of the contour-sensitive activity was defined as the time when the activity exceeded the baseline by 2 STD. Despite the modified criteria, the selected sensors for the radial and quadrant contours were located in the same middle posterior part of the measurement helmet as the selected sensors for the tangential contours.

The spatial patterns of the current estimates for the contour vs. no-contour effects were rather similar for all contour types (Figure 5). However, the effects reached

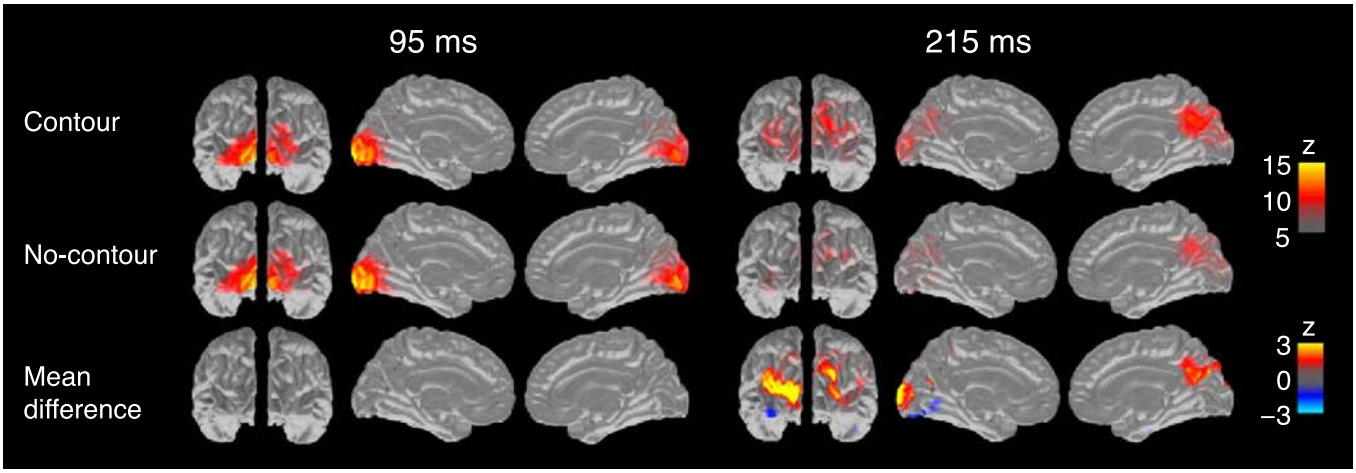

Figure 3. Patterns of cortical activity 95 ms (left) and 215 ms (right) after stimulus onset. Grand average source estimates are given for responses to tangential contour and no-contour stimuli and for their differences (contour-sensitive responses).

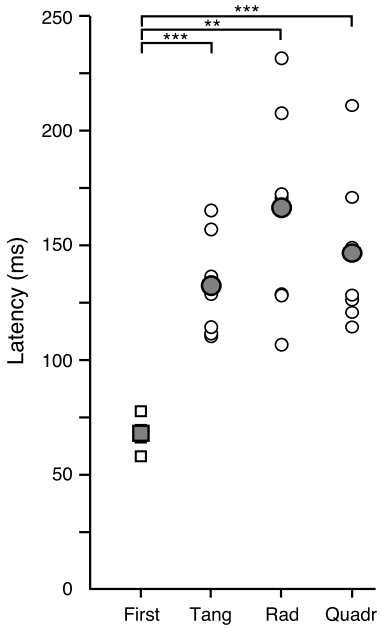

Figure 4. Latencies of the emergence of the first cortical response (squares) and contour-sensitive responses (circles) for each subject and for different contour types (Tang—tangential, Rad—radial, and Quadr—quadrant). Filled symbols indicate the mean latencies.

their maximum 25–30 ms later for the radial and quadrant contours as compared with the tangential contours.

Reaction times

The reaction times for discriminating between the contour vs. no-contour stimuli were the shortest, about 550 ms, to the tangential stimuli and ~50 ms longer to radial and quadrant stimuli ($p < 0.01$ for both categories; Figure 6). The RTs to contour vs. no-contour stimuli did not differ systematically within any category (the RTs were measured in a block design similar to the MEG experiments, yielding three different measurements for identical no-contour stimuli). The RTs did not correlate statistically significantly with response latencies.

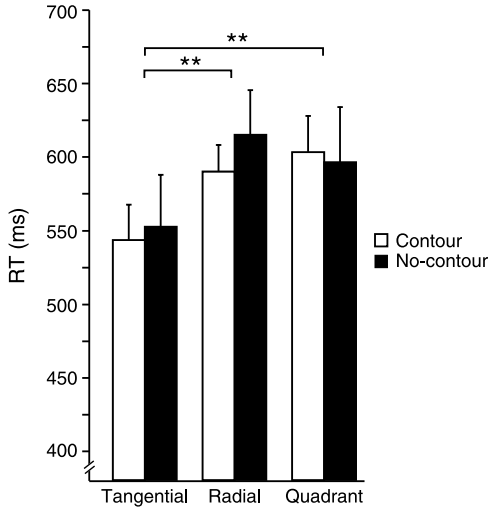

Figure 6. Mean ±*SEM* discrimination reaction times for different contour types across all subjects. The subjects had to report whether the presented stimulus contained a contour or not (**$p < 0.01$).

Discussion

Our goal was to determine the dynamics of human cortical activation that differentiates Gabor patch stimuli forming circular contours from those forming random patterns. This distinction is related to differentiation

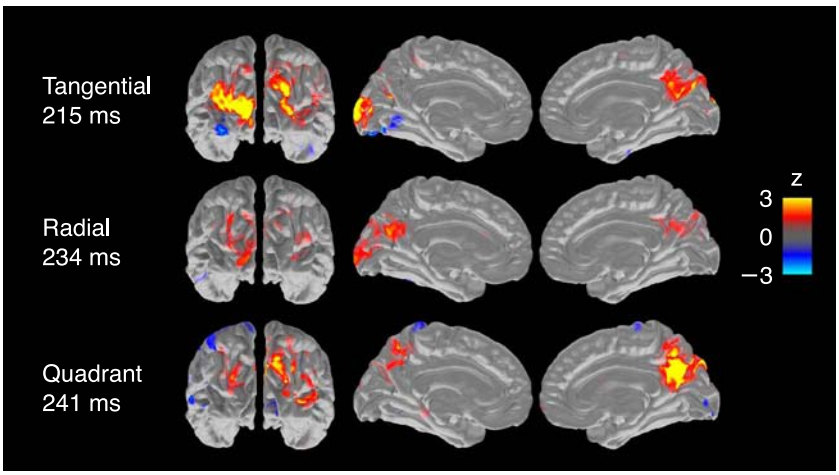

Figure 5. Effect of contour type. Grand average differences (contour vs. no-contour) of the source estimates of responses to tangential, radial, and quadrant contour types.

between global vs. local effects in visual processing. We found early responses that were identical to contour and no-contour stimuli, and later responses that were sensitive to contours and thus to the global form. The early responses were generated around the primary visual cortex, whereas the later responses arose from the more lateral and dorsal occipital and parietal regions. These two stages of processing are in good agreement with the behavioral results by Hess et al. (2001), demonstrating that the process of linking the elements to a contour is slow compared with the detection of the constituent elements.

Time course of contour integration

When the local elements were oriented tangentially to the global contour, the difference emerged on average at 130 ms after the stimulus onset, in a good agreement with previous evoked potential studies on visual segmentation and grouping in which detectable contours modulated visual evoked potentials (VEPs) over the posterior scalp, starting around 150 ms after stimulus onset (measured as the mean latency of N1 response; Mathes, Trenner, & Fahle, 2006). Similarly as in our study, the effect was strongest for contours in which the local elements were aligned along a global contour. Correspondingly, potentials evoked by random and circular Glass patterns begin with similar early responses and start to differ around 130 ms (Ohla, Busch, Dahlem, & Herrmann, 2005; Pei, Pettet, Vildavski, & Norcia, 2005). Similar posterior responses have been found 100–300 ms after the presentation of stimuli that contain a texture border defined by luminance, orientation, motion, or stereoscopic depth (Bach & Meigen, 1997; Fahle, Quenzer, Braun, & Spang, 2003) or when visual elements are grouped by similarity (Han, Song, Ding, Yund, & Woods, 2001).

Cortical responses specific to, e.g., faces and letter strings often peak as early as at 150 ms (Allison, McCarthy, Nobre, Puce, & Belger, 1994; Tarkiainen, Cornelissen, & Salmelin, 2002), and both reaction time and VEP recordings imply that 150 ms is enough for the visual processing required for high-level categorization (Fabre-Thorpe, Delorme, Marlot, & Thorpe, 2001; Thorpe, Fize, & Marlot, 1996). Therefore, the contour-sensitive responses emerging at 130–150 ms and peaking around 270 ms most likely do not reflect the first steps of integrating local information to global shapes. More likely interpretations of the observed contour-sensitive activity are discussed below in the context of the involved cortical regions.

Location of cortical activity

The center of the early non-specific activity agrees, on the basis of Talairach coordinates, with the V1 cortex. This site around the calcarine sulcus did not differentiate between contour and no-contour stimuli at any latency.

Contour-sensitive activations occurred around the posterior parieto-occipital (PO) cortex, with the strongest effects medially at the PO sulcus and precuneus, and postero-laterally in areas spanning from cuneus to middle and superior occipital gyri.

Linking of neighboring visual elements to a perceptual whole could rely either on interactions in V1 (Li, Piëch, & Gilbert, 2006) or on extrastriate processes. Although the relatively late timing and the extra-striate location of the most prominent contour-sensitive response do not exclude contour integration processes occurring within the primary visual cortex, they emphasize the role of the extra-striate areas in the formation of global visual percepts.

The site of the present contour-sensitive effects around the PO sulcus, a likely functional homologue of macaque area V6/V6a (Colby, Gattass, Olson, & Gross, 1988; Galletti, Battaglini, & Fattori, 1991; Pitzalis et al., 2006), is involved in a wide range of cortical processes (Cavanna & Trimble, 2006). The PO region responds to basic visual stimuli and eye blinking (Bristow, Frith, & Rees, 2005; Dechent & Frahm, 2003; Hari, Salmelin, Tissari, Kajola, & Virsu, 1994; Portin, Salenius, Salmelin, & Hari, 1998; Vanni, Tanskanen, Seppä, Uutela, & Hari, 2001), and it is the most prominent generator of the posterior alpha rhythm (Hari & Salmelin, 1997), the level of which is inversely related to the saliency of perceived visual objects (Vanni, Revonsuo, & Hari, 1997). Closely related to our study, activity in the PO region covaries with the number of attention switches between local and global elements of visual objects (Fink et al., 1997). Patients with lesions in the parieto-occipital cortex, typically bilaterally, fail to perceive more than one object at a time, having a difficulty in integrating elements of the visual field and switching between them (Rizzo, 1993). For example, reading is difficult since letters constituting words are perceived separately. All these findings agree with the role of the PO region in the formation of global visual percepts.

The more postero-lateral contour-sensitive activations spanned from cuneus to middle and superior occipital gyri and thus across several functional areas, with the largest overlap with area V3a. Besides visual motion (Tootell et al., 1997), human V3a could be involved in processing of visual objects at a level independent of the type of the visual cues defining an object (Grill-Spector, Kushnir, Edelman, Itzchak, & Malach, 1998).

Schira, Fahle, Donner, Kraft, and Brandt (2004) observed strongest contour-related modulation of fMRI signals in V3a. Similarly, Mendola, Dale, Fischl, Liu, and Tootell (1999) showed that V3a and other crudely retinotopic areas were responsive to illusory contours, the perception of which requires integration of local elements. On the other hand, both early retinotopic areas and higher occipitotemporal areas (V1, V2, VP, V4v, LOC) responded more strongly to arrays of Gabor patches

that contained a global contour than to arrays that did not (Altmann et al., 2003). When similar stimuli were presented in an adaptation paradigm, sensitivity to contours was again found in many visual areas (Kourtzi et al., 2003). Interestingly, V1 showed significant modulations for peripheral but not for central visual field, whereas V2 showed an opposite pattern. The effect was explained by differences in receptive field sizes between these areas. A similar interpretation could be possible for the partial, but not full overlap, of the regions detected in our study vs. in the earlier fMRI studies. Another contributing factor is that MEG and fMRI may reflect partly different aspects of neuronal activity (for an example, see Furey et al., 2006).

Effect of local orientation

According to behavioral studies, finding a contour (path of elements) among randomly distributed elements is most efficient when the local elements are aligned along the contour (Bonneh & Sagi, 1998; Field et al., 1993; Kovács & Julesz, 1993; Pettet et al., 1998; Saarinen & Levi, 2001; Saarinen et al., 1997). Accordingly, we found that the most consistent contour-sensitive cortical effects were produced by the full circular contours in which the local elements were oriented tangentially to the global contour; the effects were weaker when the local orientations were radial or when tangential elements formed only quadrant contours. Besides indicating matching local and global orientations, this result might reflect enhanced processing of concentric patterns (Dumoulin & Hess, 2007; Kurki & Saarinen, 2004; Wilkinson et al., 2000).

In line with these data, the RTs for contour–no-contour discrimination were in this study shortest when the local elements were aligned along the global contour, and the contour formed a full circle. The range of the discrimination RTs (ca. 550–620 ms) is very close to that reported by Beaudot and Mullen (2001) for a similar task.

We note that it is possible that cortical processing of contours might be reflected in oscillatory brain activity as well, but in this study we focused our analysis on the timing and location of evoked cortical responses.

Conclusions

We describe distinct stages of cortical processes involved in the fundamental operation of integrating local visual information to a global percept. The first responses, emerging in the region of the primary visual cortex, did not differentiate between contours and random arrays of visual elements. On the contrary, later responses—emerging around 130 ms in the PO region and areas spanning from cuneus to middle and superior occipital gyri—were clearly stronger to the contour stimuli. Our findings emphasize the role of these extra-striate brain areas in the formation of integrated visual percepts, including global shapes.

Acknowledgments

We thank Matti Hämäläinen for providing the software for cortically constrained current estimates, Risto Näsänen for advice on stimulus calibration, and Jaakko Järvinen and Simo Vanni for comments on the manuscript.

This research was supported by the Academy of Finland (National Programme for Centres of Excellence 2006-2011).

Commercial relationships: none.
Corresponding author: Topi Tanskanen.
Email: topi.tanskanen@tkk.fi.
Address: Brain Research Unit, Low Temperature Laboratory, Helsinki University of Technology, PO Box 5100, 02015 TKK, Finland.

References

Allison, T., McCarthy, G., Nobre, A., Puce, A., & Belger, A. (1994). Human extrastriate visual cortex and the perception of faces, words, numbers, and colors. *Cerebral Cortex, 4,* 544–554. [PubMed]

Altmann, C. F., Bülthoff, H. H., & Kourtzi, Z. (2003). Perceptual organization of local elements into global shapes in the human visual cortex. *Current Biology, 13,* 342–349. [PubMed] [Article]

Bach, M., & Meigen, T. (1997). Similar electrophysiological correlates of texture segregation induced by luminance, orientation, motion and stereo. *Vision Research, 37,* 1409–1414. [PubMed]

Beaudot, W. H., & Mullen, K. T. (2001). Processing time of contour integration: The role of colour, contrast, and curvature. *Perception, 30,* 833–853. [PubMed]

Bonneh, Y., & Sagi, D. (1998). Effects of spatial configuration on contrast detection. *Vision Research, 38,* 3541–3553. [PubMed]

Braun, J. (1999). On the detection of salient contours. *Spatial Vision, 12,* 211–225. [PubMed]

Bristow, D., Frith, C., & Rees, G. (2005). Two distinct neural effects of blinking on human visual processing. *Neuroimage, 27,* 136–145. [PubMed]

Cavanna, A. E., & Trimble, M. R. (2006). The precuneus: A review of its functional anatomy and behavioural correlates. *Brain, 129,* 564–583. [PubMed]

Colby, C. L., Gattass, R., Olson, C. R., & Gross, C. G. (1988). Topographical organization of cortical afferents to extrastriate visual area PO in the macaque: A dual tracer study. *Journal of Comparative Neurology, 269,* 392–413. [PubMed]

Dale, A. M., Fischl, B., & Sereno, M. I. (1999). Cortical surface-based analysis. I. Segmentation and surface reconstruction. *Neuroimage, 9,* 179–194. [PubMed]

Dale, A. M., Liu, A. K., Fischl, B. R., Buckner, R. L., Belliveau, J. W., Lewine, J. D., et al. (2000). Dynamic statistical parametric mapping: Combining fMRI and MEG for high-resolution imaging of cortical activity. *Neuron, 26,* 55–67. [PubMed] [Article]

Dechent, P., & Frahm, J. (2003). Characterization of the human visual V6 complex by functional magnetic resonance imaging. *European Journal of Neuroscience, 17,* 2201–2211. [PubMed]

Dumoulin, S. O., & Hess, R. F. (2007). Cortical specialization for concentric shape processing. *Vision Research, 47,* 1608–1613. [PubMed]

Fabre-Thorpe, M., Delorme, A., Marlot, C., & Thorpe, S. (2001). A limit to the speed of processing in ultra-rapid visual categorization of novel natural scenes. *Journal of Cognitive Neuroscience, 13,* 171–180. [PubMed]

Fahle, M., Quenzer, T., Braun, C., & Spang, K. (2003). Feature-specific electrophysiological correlates of texture segregation. *Vision Research, 43,* 7–19. [PubMed]

Field, D. J., Hayes, A., & Hess, R. F. (1993). Contour integration by the human visual system: Evidence for a local "association field". *Vision Research, 33,* 173–193. [PubMed]

Fink, G. R., Halligan, P. W., Marshall, J. C., Frith, C. D., Frackowiak, R. S., & Dolan, R. J. (1997). Neural mechanisms involved in the processing of global and local aspects of hierarchically organized visual stimuli. *Brain, 120,* 1779–1791. [PubMed]

Fischl, B., Sereno, M. I., Tootell, R. B., & Dale, A. M. (1999). High-resolution intersubject averaging and a coordinate system for the cortical surface. *Human Brain Mapping, 8,* 272–284. [PubMed]

Furey, M. L., Tanskanen, T., Beauchamp, M. S., Avikainen, S., Uutela, K., Hari, R., et al. (2006). Dissociation of face-selective cortical responses by attention. *Proceedings of the National Academy of Sciences of the United States of America, 103,* 1065–1070. [PubMed] [Article]

Galletti, C., Battaglini, P. P., & Fattori, P. (1991). Functional properties of neurons in the anterior bank of the parieto-occipital sulcus of the macaque monkey. *European Journal of Neuroscience, 3,* 452–461. [PubMed]

Grill-Spector, K., Kushnir, T., Edelman, S., Itzchak, Y., & Malach, R. (1998). Cue-invariant activation in object-related areas of the human occipital lobe. *Neuron, 21,* 191–202. [PubMed] [Article]

Hämäläinen, M., Hari, R., Ilmoniemi, R. J., Knuutila, J., & Lounasmaa, O. V. (1993). Magnetoencephalography—Theory, instrumentation, and applications to noninvasive studies of the working human brain. *Reviews of Modern Physics, 65,* 413–497.

Han, S., Song, Y., Ding, Y., Yund, E. W., & Woods, D. L. (2001). Neural substrates for visual perceptual grouping in humans. *Psychophysiology, 38,* 926–935. [PubMed]

Hari, R. (1990). The neuromagnetic method in the study of the human auditory cortex. In F. Grandori, M. Hoke, & G. L. Romani (Eds.), *Auditory evoked magnetic fields and electric potentials* (vol. 6, pp. 222–282). Basel: Karger.

Hari, R., & Salmelin, R. (1997). Human cortical oscillations: A neuromagnetic view through the skull. *Trends in Neurosciences, 20,* 44–49. [PubMed]

Hari, R., Salmelin, R., Tissari, S. O., Kajola, M., & Virsu, V. (1994). Visual stability during eyeblinks. *Nature, 367,* 121–122. [PubMed]

Hess, R. F., Beaudot, W. H., & Mullen, K. T. (2001). Dynamics of contour integration. *Vision Research, 41,* 1023–1037. [PubMed]

Hess, R. F., Hayes, A., & Field, D. J. (2003). Contour integration and cortical processing. *The Journal of Physiology, 97,* 105–119. [PubMed]

Hubel, D. H., & Wiesel, T. N. (1974). Uniformity of monkey striate cortex: A parallel relationship between field size, scatter, and magnification factor. *Journal of Comparative Neurology, 158,* 295–305. [PubMed]

Kapadia, M. K., Ito, M., Gilbert, C. D., & Westheimer, G. (1995). Improvement in visual sensitivity by changes in local context: Parallel studies in human observers and in V1 of alert monkeys. *Neuron, 15,* 843–856. [PubMed] [Article]

Knierim, J. J., & van Essen, D. C. (1992). Neuronal responses to static texture patterns in area V1 of the alert macaque monkey. *Journal of Neurophysiology, 67,* 961–980. [PubMed]

Koffka, K. (1935). *Principles of Gestalt psychology*. New York: Harcourt.

Kourtzi, Z., Tolias, A. S., Altmann, C. F., Augath, M., & Logothetis, N. K. (2003). Integration of local features into global shapes: Monkey and human FMRI studies. *Neuron, 37,* 333–346. [PubMed] [Article]

Kovács, I., & Julesz, B. (1993). A closed curve is much more than an incomplete one: Effect of closure in figure-ground segmentation. *Proceedings of the National Academy of Sciences of the United States of America, 90,* 7495–7497. [PubMed] [Article]

Kurki, I., & Saarinen, J. (2004). Shape perception in human vision: Specialized detectors for concentric spatial structures? *Neuroscience Letters, 360,* 100–102. [PubMed]

Lamme, V. A. (1995). The neurophysiology of figure-ground segregation in primary visual cortex. *Journal of Neuroscience, 15,* 1605–1615. [PubMed] [Article]

Li, W., Piëch, V., & Gilbert, C. D. (2006). Contour saliency in primary visual cortex. *Neuron, 50,* 951–962. [PubMed] [Article]

Lin, F. H., Belliveau, J. W., Dale, A. M., & Hämäläinen, M. S. (2006). Distributed current estimates using cortical orientation constraints. *Human Brain Mapping, 27,* 1–13. [PubMed]

Marcelja, S. (1980). Mathematical description of the responses of simple cortical cells. *Journal of the Optical Society of America, 70,* 1297–1300. [PubMed]

Mathes, B., Trenner, D., & Fahle, M. (2006). The electrophysiological correlate of contour integration is modulated by task demands. *Brain Research, 1114,* 98–112. [PubMed]

Mendola, J. D., Dale, A. M., Fischl, B., Liu, A. K., & Tootell, R. B. (1999). The representation of illusory and real contours in human cortical visual areas revealed by functional magnetic resonance imaging. *Journal of Neuroscience, 19,* 8560–8572. [PubMed] [Article]

Ohla, K., Busch, N. A., Dahlem, M. A., & Herrmann, C. S. (2005). Circles are different: The perception of Glass patterns modulates early event-related potentials. *Vision Research, 45,* 2668–2676. [PubMed]

Okada, Y. C., Wu, J., & Kyuhou, S. (1997). Genesis of MEG signals in a mammalian CNS structure. *Electroencephalography and Clinical Neurophysiology, 103,* 474–485. [PubMed]

Packer, O., Diller, L. C., Verweij, J., Lee, B. B., Pokorny, J., Williams, D. R., et al. (2001). Characterization and use of a digital light projector for vision research. *Vision Research, 41,* 427–439. [PubMed]

Parkkonen, L. T., Simola, J. T., Tuoriniemi, J., & Ahonen, A. I. (1999). An interference suppression system for multichannel magnetic field detector arrays. In T. Yoshimoto, M. Kotani, S. Kuriki, H. Karibe, & N. Nakasato (Eds.), *Recent advances in biomagnetism: Proceedings of the 11th international conference on biomagnetism* (p. 13). Sendai: Tohoku University Press.

Pei, F., Pettet, M. W., Vildavski, V. Y., & Norcia, A. M. (2005). Event-related potentials show configural specificity of global form processing. *Neuroreport, 16,* 1427–1430. [PubMed]

Pettet, M. W., McKee, S. P., & Grzywacz, N. M. (1998). Constraints on long range interactions mediating contour detection. *Vision Research, 38,* 865–879. [PubMed]

Pitzalis, S., Galletti, C., Huang, R. S., Patria, F., Committeri, G., Galati, G., et al. (2006). Wide-field retinotopy defines human cortical visual area v6. *Journal of Neuroscience, 26,* 7962–7973. [PubMed] [Article]

Portin, K., Salenius, S., Salmelin, R., & Hari, R. (1998). Activation of the human occipital and parietal cortex by pattern and luminance stimuli: Neuromagnetic measurements. *Cerebral Cortex, 8,* 253–260. [PubMed] [Article]

Rizzo, M. (1993). 'Bálint's syndrome' and associated visuospatial disorders. *Bailliere's Clinical Neurology, 2,* 415–437.

Roelfsema, P. R. (2006). Cortical algorithms for perceptual grouping. *Annual Review of Neuroscience, 29,* 203–227. [PubMed]

Rossi, A. F., Desimone, R., & Ungerleider, L. G. (2001). Contextual modulation in primary visual cortex of macaques. *Journal of Neuroscience, 21,* 1698–1709. [PubMed] [Article]

Saarinen, J., & Levi, D. M. (2001). Integration of local features into a global shape. *Vision Research, 41,* 1785–1790. [PubMed]

Saarinen, J., Levi, D. M., & Shen, B. (1997). Integration of local pattern elements into a global shape in human vision. *Proceedings of the National Academy of Sciences of the United States of America, 94,* 8267–8271. [PubMed] [Article]

Sasaki, Y. (2007). Processing local signals into global patterns. *Current Opinion in Neurobiology, 17,* 132–139. [PubMed]

Schira, M. M., Fahle, M., Donner, T. H., Kraft, A., & Brandt, S. A. (2004). Differential contribution of early visual areas to the perceptual process of contour processing. *Journal of Neurophysiology, 91,* 1716–1721. [PubMed] [Article]

Tarkiainen, A., Cornelissen, P. L., & Salmelin, R. (2002). Dynamics of visual feature analysis and object-level processing in face versus letter-string perception. *Brain, 125,* 1125–1136. [PubMed] [Article]

Taulu, S., Kajola, M., & Simola, J. (2004). Suppression of interference and artifacts by the Signal Space Separation Method. *Brain Topography, 16,* 269–275. [PubMed]

Thorpe, S., Fize, D., & Marlot, C. (1996). Speed of processing in the human visual system. *Nature, 381,* 520–522. [PubMed]

Tootell, R. B., Mendola, J. D., Hadjikhani, N. K., Ledden, P. J., Liu, A. K., Reppas, J. B., et al. (1997). Functional analysis of V3A and related areas in human visual cortex. *Journal of Neuroscience, 17,* 7060–7078. [PubMed] [Article]

Vanni, S., Revonsuo, A., & Hari, R. (1997). Modulation of the parieto-occipital alpha rhythm during object detection. *Journal of Neuroscience, 17,* 7141–7147. [PubMed] [Article]

Vanni, S., Tanskanen, T., Seppä, M., Uutela, K., & Hari, R. (2001). Coinciding early activation of the human primary visual cortex and anteromedial cuneus. *Proceedings of the National Academy of Sciences of the United States of America, 98,* 2776–2780. [PubMed] [Article]

Wilkinson, F., James, T. W., Wilson, H. R., Gati, J. S., Menon, R. S., & Goodale, M. A. (2000). An fMRI study of the selective activation of human extrastriate form vision areas by radial and concentric gratings. *Current Biology, 10,* 1455–1458. [PubMed] [Article]

Zipser, K., Lamme, V. A., & Schiller, P. H. (1996). Contextual modulation in primary visual cortex. *Journal of Neuroscience, 16,* 7376–7389. [PubMed] [Article]